Two-dimensional complete photonic gaps from layered periodic structures containing anisotropic left-handed metamaterials

Shulin Sun, Xueqin Huang, and Lei Zhou*
Surface Physics Laboratory (State Key Laboratory) and Physics Department, Fudan University, Shanghai 200433, China
(Received 14 December 2006; published 6 June 2007)

We demonstrate that a two-dimensional *complete* photonic band-gap (PBG) can be realized in a layered periodic structure with a double-layer unit cell containing an *anisotropic* left-handed metamaterial layer. A set of criteria is derived for the geometric and material parameters to realize a two-dimensional complete PBG in such systems, and a detailed phase diagram is given. We discuss the underlying physics of the mechanism and illustrate the complete band-gap effects with several concrete examples.

DOI: 10.1103/PhysRevE.75.066602 PACS number(s): 42.70.Qs, 41.20.Jb, 78.67.Pt, 78.20.Bh

I. INTRODUCTION

Conventional photonic band-gap (PBG) material is a type of artificial composite with periodically modulated dielectric constant, and the photonic gap is opened via the Bragg scattering mechanism [1,2]. Usually, a periodic modulation along one direction only yields a partial gap along that particular direction. To realize a two-dimensional (2D) or 3D complete PBG, one needs to construct photonic crystals (PhC's) with dielectric functions modulated periodically in two or three dimensions [3–5]. However, such systems are not easy to fabricate due to the complexities of the structure. Although it was shown that a 1D PhC with appropriate geometric and material parameters could provide an omnidirectional reflection, such an effect is not originated from a 3D complete PBG [6,7].

Left-handed metamaterial (LHM) is another type of artificial composite which has simultaneously negative permittivity and permeability and, in turn, a negative refractive index [8]. LHM samples functioning in microwave frequency regime have been successfully fabricated in the laboratory [9], and many interesting electromagnetic (EM) characteristics have been proposed or discovered based on such novel materials [8,9]. In particular, PhC's combining LHM and ordinary materials were shown to display several extraordinary PBG properties, which do not exist in conventional PhC's [10,11]. For example, a new type of PBG corresponding to a vanishing (volume) averaged refractive index, denoted by the zero-$\bar{n}$ gap, can be realized in a layered system combining both positive- and negative-index material, which is robust against weak disorder and lattice scaling and possesses many other unusual properties [10]. Recently, Shadrivov *et al.* argued that a 3D complete PBG could be achieved in a 1D layered system consisting of isotropic LHM layers with specific material and structural parameters [11]. This is quite intriguing at first sight, since one naturally wonders how the light propagation is stopped along the other two dimensions *without* Bragg scatterings. It turns out that the unusual properties of a LHM waveguide are the keys to understand such a surprising result [11,12].

We note that the proposed structure in Ref. [11] requires an *isotropic* LHM sample, which is relatively hard to obtain since most of the LHM samples designed to date are *anisotropic* in nature. In this paper, we extend the ideas presented in Ref. [11] to investigate the possibilities of realizing a complete PBG in a layered system containing *anisotropic transparent* LHM layers. The anisotropic metamaterials have attracted considerable attention recently due to many unexpected optical properties discovered in such systems [13–17]. Since the anisotropy introduces additional complexities to the problem, in the present paper, we only focus on the possibilities of realizing a 2*D* complete PBG, which is relatively easy to tackle. We present our work in the following way. In Sec. II, we derive a set of criteria to facilitate researchers to seek appropriate parameters that support a 2D complete PBG in such a system and then present in Sec. III a phase diagram for the permitted structural and material parameters, as well as a general discussion of the underlying mechanism for opening the complete PBG. We find that the isotropic case discussed in Ref. [11] has been automatically included in our general considerations. We then study several examples to illustrate the complete gap effects in Sec. IV and summarize our work in the last section.

II. CRITERIA TO REALIZE A 2D COMPLETE PBG

A. General formulas

The system we study is a 1D periodic layered structure with a double-layer unit cell consisting of an air layer of a thickness d_1 and an anisotropic LHM layer of a thickness d_2. The latter is characterized by a permittivity tensor

$$\vec{\vec{\varepsilon}} = \begin{pmatrix} \varepsilon_{xx} & 0 & 0 \\ 0 & \varepsilon_{yy} & 0 \\ 0 & 0 & \varepsilon_{zz} \end{pmatrix}$$

and a permeability tensor

$$\vec{\vec{\mu}} = \begin{pmatrix} \mu_{xx} & 0 & 0 \\ 0 & \mu_{yy} & 0 \\ 0 & 0 & \mu_{zz} \end{pmatrix}$$

where the z axis is chosen normal to each layer. In this paper, we only consider the possibilities of realizing a 2D complete

*Author to whom correspondence should be addressed. Electronic address: phzhou@fudan.edu.cn

PBG. Thus, we confine the light propagation directions in the x-z plane and consider two independent polarizations—namely, the transverse-electric (TE) mode with $\vec{E}=E\hat{y}$ and the transverse-magnetic (TM) mode with $\vec{B}=B\hat{y}$. According to the Bloch theory, an eigen-EM wave inside a PhC should be a Bloch wave with a Bloch wave vector $\vec{K}=K_z\hat{z}+K_x\hat{x}$. With the help of the transfer matrix method, we find that K_z is determined by the trace of a transfer matrix,

$$\mathrm{Tr}[T(\omega,K_x)]=2\cos(K_z a), \tag{1}$$

with $a=(d_1+d_2)$ being the lattice constant. The transfer matrix is a function of the frequency ω and the parallel wave vector K_x, which is conserved throughout the structures. For a TE mode, simple calculations show that

$$\mathrm{Tr}[T_{TE}(\omega,K_x)]=\frac{1}{4}\{(2+\Delta+\Delta^{-1})[e^{i(k_{2z}d_2+k_{1z}d_1)} + e^{-i(k_{2z}d_2+k_{1z}d_1)}]+(2-\Delta-\Delta^{-1})[e^{i(k_{2z}d_2-k_{1z}d_1)} + e^{-i(k_{2z}d_2-k_{1z}d_1)}]\} \tag{2}$$

where $k_{1z}=\sqrt{(\omega/c)^2-K_x^2}$, $k_{2z}=\sqrt{\varepsilon_{yy}\mu_{xx}(\omega/c)^2-(\mu_{xx}/\mu_{zz})K_x^2}$, and $\Delta=k_{2z}/(\mu_{xx}k_{1z})$ [18]. For a TM mode, $\mathrm{Tr}[T_{TM}(\omega,K_x)]$ takes exactly the same form as Eq. (2), with only μ_{xx}, μ_{zz}, and ε_{yy} substituted by ε_{xx}, ε_{zz}, and μ_{yy}, correspondingly. Equation (1) immediately suggests that when the condition

$$|\mathrm{Tr}[T_{TE}(\omega,K_x)]|>2,$$

$$|\mathrm{Tr}[T_{TM}(\omega,K_x)]|>2 \quad (-\infty<K_x<\infty) \tag{3}$$

is satisfied, no propagating mode is allowed inside the system so that a 2D complete PBG opens. In what follows, we will examine the condition (3) in detail, to search for the criteria imposed on the material parameters $\vec{\vec{\mu}}$ and $\vec{\vec{\varepsilon}}$ and the structural parameters d_1/λ, d_2/λ (where λ is the gap wavelength). Due to the symmetry between TE and TM polarizations, we only consider the case of TE polarization in the following discussions.

We first consider in Sec. II B the situation that all elements of $\vec{\vec{\varepsilon}}$ and $\vec{\vec{\mu}}$ tensors are negative and then demonstrate in Sec. II C that structures containing ordinary materials (i.e., all elements of $\vec{\vec{\varepsilon}}$ and $\vec{\vec{\mu}}$ tensors are positive) cannot support a 2D complete PBG. We will not consider the cases that some elements of $\vec{\vec{\varepsilon}}$ and $\vec{\vec{\mu}}$ tensors are negative while some others are positive, since such metamaterials are inherently *opaque* in some situations and thus become less interesting for the present problem.

B. Situation of $\vec{\vec{\varepsilon}}$ and $\vec{\vec{\mu}}<0$

We only consider the case of $\varepsilon_{yy}\mu_{zz}>1$ (i.e., the LHM layer is optically dense), since the case of $\varepsilon_{yy}\mu_{zz}<1$ (i.e., the LHM layer is optically sparse) yields similar conclusions. Defining two critical values for K_x, $k_c^1=\omega/c$ and $k_c^2=\sqrt{\varepsilon_{yy}\mu_{zz}}\omega/c$, we now separately consider the behaviors of $\mathrm{Tr}(T)$ (subscript "TE" is omitted in the following discussions) for K_x located inside the following three regions.

(I) When $0\le K_x<k_c^1$, both k_{1z} and k_{2z} are real, and we call it a propagating wave (PW) region.

(II) When $k_c^1<K_x<k_c^2$, k_{1z} is imaginary but k_{2z} is real, and we call it a guided surface wave (GSW) region since the EM wave is guided inside the metamaterial layer.

(III) When $K_x>k_c^2$, both k_{1z} and k_{2z} are imaginary, and we call it a surface plasmon polariton (SPP) region.

We first consider the SPP region. Setting $k_{1z}=i\alpha$ and $k_{2z}=i\beta$, we obtain

$$\mathrm{Tr}(T)=\frac{1}{4}\{(2+\Delta+\Delta^{-1})[e^{-(\alpha d_1+\beta d_2)}+e^{(\alpha d_1+\beta d_2)}] + (2-\Delta-\Delta^{-1})[e^{-(\alpha d_1-\beta d_2)}+e^{(\alpha d_1-\beta d_2)}]\}, \tag{4}$$

with $\Delta=\frac{\beta}{\mu_{xx}\alpha}<0$. Considering the fact that $\Delta+\Delta^{-1}<-2$ [19], we find that $\mathrm{Tr}(T)$ tends to $-\infty$ as $K_x\to\infty$. *This property indicates that we must ensure* $\mathrm{Tr}(T)<-2$ *for all* K_x *in order to get a complete PBG.* Considering the variation region of $\Delta(\in(0,-1/\sqrt{\mu_{xx}\mu_{zz}}))$ within the entire SPP region, we find that the condition to ensure $\mathrm{Tr}(T)<-2$ is

$$\mu_{xx}\mu_{zz}>1. \tag{5}$$

We next consider the PW region where we have

$$\mathrm{Tr}(T)=2\cos(k_{1z}d_1-k_{2z}d_2) - (\Delta+\Delta^{-1}+2)\sin k_{1z}d_1\sin k_{2z}d_2. \tag{6}$$

Apparently, to ensure $\mathrm{Tr}(T)<-2$ in this region, we need the Bragg condition

$$k_{1z}d_1-k_{2z}d_2=-m\pi \quad (m=1,3,5,\ldots). \tag{7}$$

It is interesting to note that one must create an *odd-numbered Bragg gap* in order to realize a complete PBG. This is a unique property imposed by the *negative* index of the metamaterial which dictates $\mathrm{Tr}(T)\to-\infty$ as $K_x\to\infty$. Later after considering the criteria in the GSW region, we further show that actually *only the mode with* $m=1$ is eligible to guarantee that $\mathrm{Tr}(T)<-2$ throughout the whole three regions.

In the normal incidence case (i.e., $K_x=0$), Eq. (7) becomes (setting $m=1$)

$$\frac{\omega}{c}d_1-\sqrt{\varepsilon_{yy}\mu_{xx}}\frac{\omega}{c}d_2=\bar{n}\frac{\omega}{c}(d_1+d_2)=-\pi, \tag{8}$$

where $\bar{n}=(d_1-\sqrt{\varepsilon_{yy}\mu_{xx}}d_2)/(d_1+d_2)$ is the volume-averaged refractive index for light traveling along the z direction (recalling that ε_{yy}, $\mu_{xx}<0$ so that the refractive index in this medium is negative). Although it was shown that a layered system possessing a zero-$\bar{n}$ gap supports an omnidirectional reflection [17,20], here we rigorously demonstrate that such a gap is *not* a complete PBG [21].

When K_x changes from 0 to k_c^1 within the PW region, we find $k_{1z}d_1$, $k_{2z}d_2$, and Δ to locate inside

$$0 < k_{1z}d_1 < \frac{\omega}{c}d_1,$$

$$\sqrt{\varepsilon_{yy}\mu_{xx} - \mu_{xx}/\mu_{zz}}\frac{\omega}{c}d_2 < k_{2z}d_2 < \sqrt{\varepsilon_{yy}\mu_{xx}}\frac{\omega}{c}d_2,$$

$$-\infty < \Delta < -\sqrt{\varepsilon_{yy}/\mu_{xx}}. \quad (9)$$

According to Eq. (6) and employing the fact that $\Delta+\Delta^{-1}+2<0$ [19], we find that the conditions to guarantee $\mathrm{Tr}(T)<-2$ within this region are

$$\sin k_{1z}d_1 > 0, \quad \sin k_{2z}d_2 < 0, \quad \varepsilon_{yy}/\mu_{xx} > 1. \quad (10)$$

Equation (10) implies that $k_{1z}d_1 \in (0,\pi)$ and $k_{2z}d_2 \in (\pi,2\pi)$. Considering the upper and lower boundaries of $k_{1z}d_1$ and $k_{2z}d_2$ as shown in Eq. (9), we find that Eq. (10) can be further simplified to the following set of transparent restrictions imposed on the parameter and structural parameters:

$$d_1 < \lambda/2,$$

$$\frac{\lambda}{2}\sqrt{\mu_{zz}/[\mu_{xx}(\varepsilon_{yy}\mu_{zz}-1)]} < d_2 < \lambda/\sqrt{\varepsilon_{yy}\mu_{xx}}, \varepsilon_{yy}\mu_{zz} > 4/3,$$

$$\varepsilon_{yy} < \mu_{xx}. \quad (11)$$

The most difficult region turns out to be the GSW region (i.e., $k_c^1<K_x<k_c^2$). Here, k_{1z} $(=i\alpha)$ is purely imaginary and k_{2z} is real, so that we can rewrite $\mathrm{Tr}(T)$ as

$$\mathrm{Tr}(T) = -(e^{-\alpha d_1}+e^{\alpha d_1}) - 2\cosh(\alpha d_1)\left[\frac{1}{2}\left(\frac{k_{2z}}{\mu_{xx}\alpha}-\frac{\mu_{xx}\alpha}{k_{2z}}\right)\right.$$
$$\left.\times\sin(k_{2z}d_2)\tanh(\alpha d_1) - 2\cos^2(k_{2z}d_2/2)\right]. \quad (12)$$

At first sight, it seems hopeless to ensure $\mathrm{Tr}(T)<-2$ within this region, since the function $\sin(k_{2z}d_2)$ inside the brackets of Eq. (12) is an *oscillatory* function, and therefore, the second term in Eq. (12) could become positive in some situations leading to the appearances of pass bands [i.e., $|\mathrm{Tr}(T)| \le 2$]. However, a detailed examination shows that some particular structural and material parameters can help suppress this seemingly inevitable oscillation of $\mathrm{Tr}(T)$ and thus make the condition $\mathrm{Tr}(T)<-2$ satisfied within this region.

We note that at the lower edge of the GSW region (i.e., $K_x=k_c^1=\omega/c$), $k_{2z}d_2$ is an angle located inside $(\pi,2\pi)$ [see Eq. (10) and the arguments following], and at the upper edge of the GSW region (i.e., $K_x=k_c^2=\sqrt{\varepsilon_{yy}\mu_{zz}}\omega/c$) $k_{2z}d_2$ *must* be zero. Therefore, $k_{2z}d_2$ must decrease from an angle inside $(\pi,2\pi)$ to 0, as K_x changes from k_c^1 to k_c^2 within the GSW region. As a result, the function $\sin(k_{2z}d_2)$ will change its sign from negative to positive at a particular K_x value where $k_{2z}d_2=\pi$. Meanwhile, the function $\left(\frac{k_{2z}}{\mu_{xx}\alpha}-\frac{\mu_{xx}\alpha}{k_{2z}}\right)$ develops from $-\infty$ to $+\infty$ as K_x increases and changes its sign at another K_x value within the same region. Since the function $\sin(k_{2z}d_2)$ changes its sign only *once*, if we make these two transition values match, the first item in the brackets—i.e., $\frac{1}{2}\left(\frac{k_{2z}}{\mu_{xx}\alpha}-\frac{\mu_{xx}\alpha}{k_{2z}}\right)\sin(k_{2z}d_2)\tanh(\alpha d_1)$—is always positive except at the common transition K_x value. Meanwhile, at this particular K_x value requiring $k_{2z}d_2=\pi$, we find that $2\cos^2(k_{2z}d_2/2)=0$ and thus the term in brackets in Eq. (12) is equal to 0. In addition, as $K_x$leaves this common transition value, we find that the term $\frac{1}{2}\left(\frac{k_{2z}}{\mu_{xx}\alpha}-\frac{\mu_{xx}\alpha}{k_{2z}}\right)\sin(k_{2z}d_2)\tanh(\alpha d_1)$ increases more quickly than the term $2\cos^2(k_{2z}d_2/2)$. Based on all these considerations, we find that the inequality

$$\frac{1}{2}\left(\frac{k_{2z}}{\mu_{xx}\alpha}-\frac{\mu_{xx}\alpha}{k_{2z}}\right)\sin(k_{2z}d_2)\tanh(\alpha d_1) - 2\cos^2(k_{2z}d_2/2) \ge 0 \quad (13)$$

can be ensured if we match those two transition values. Equations (12) and (13) suggest that the condition of $\mathrm{Tr}(T)<-2$ can be guaranteed within this region. Simple analysis shows that matching these two K_x values requires that

$$\sqrt{\frac{\mu_{xx}^2(\mu_{zz}\varepsilon_{yy}-1)}{1+\mu_{zz}\mu_{xx}}}\frac{2d_2}{\lambda} = 1. \quad (14)$$

We emphasize that while Eq. (14) is a sufficient condition to guarantee $\mathrm{Tr}(T)<-2$ within the GSW region, it is not a necessary condition. Nevertheless, it is still helpful to guide us to search for permitted parameter values.

Conditions (5), (8), (11), and (14) form a set of sufficient criteria to facilitate our search for appropriate parameters μ_{xx}, ε_{yy}, μ_{zz}, d_1/λ, and d_2/λ, which collectively support a 2D complete PBG for the TE mode. Setting $\varepsilon_{xx}=\mu_{xx}$, $\mu_{yy}=\varepsilon_{yy}$, and $\varepsilon_{zz}=\mu_{zz}$, we then find a system to exhibit a 2D *polarization-independent* complete PBG. Similar discussions lead to the criteria for the case of $\mu_{zz}\varepsilon_{yy}<1$, which will not be repeated here.

As an example, we find the following set of parameters:

$$\mu_{xx}=\varepsilon_{xx}=-0.5, \quad \varepsilon_{yy}=\mu_{yy}=-2, \quad \mu_{zz}=\varepsilon_{zz}=-2.5,$$

$$d_1=\frac{1}{4}\lambda, \quad d_2=\frac{3}{4}\lambda, \quad (15)$$

to satisfy all the above criteria. With these parameters, we calculated $\mathrm{Tr}(T_{TE})$ as a function of K_x and depict the results

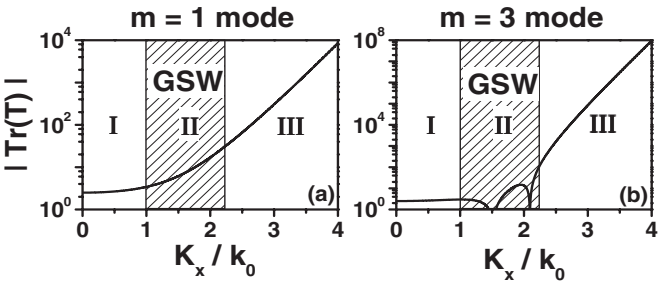

FIG. 1. $|\mathrm{Tr}(T)|$ as functions of K_x for a system with parameters (a) $\mu_{xx}=\varepsilon_{xx}=-0.5$, $\varepsilon_{yy}=\mu_{yy}=-2$, $\mu_{zz}=\varepsilon_{zz}=-2.5$, $d_1=\frac{1}{4}\lambda$, and $d_2=\frac{3}{4}\lambda$ (realizing an $m=1$ Bragg gap) and for a system with (b) $\mu_{xx}=\varepsilon_{xx}=-0.5$, $\varepsilon_{yy}=\mu_{yy}=-2$, $\mu_{zz}=\varepsilon_{zz}=-2.5$, $d_1=\frac{1}{4}\lambda$, and $d_2=\frac{7}{4}\lambda$ (realizing an $m=3$ Bragg gap). Here, I, II, and III denote the PW, GSW, and SPP regions.

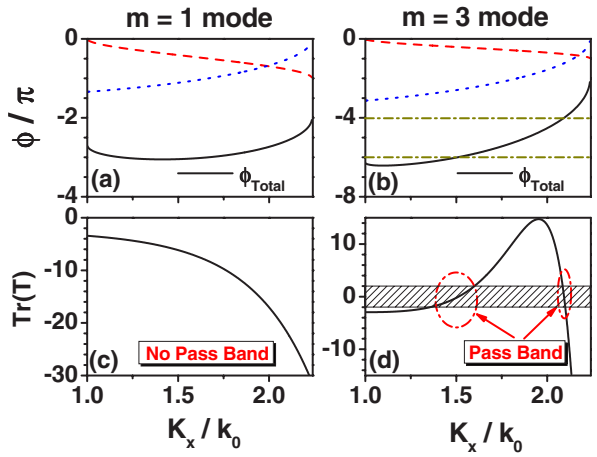

FIG. 2. (Color online) Propagation phase ϕ_P (dotted lines), reflection phase ϕ_R (dashed lines), and the total round-trip phase ϕ_{Total} (solid lines), as functions of K_x for a single anisotropic LHM waveguide with parameters given by (a) $\mu_{xx}=\varepsilon_{xx}=-0.5$, $\varepsilon_{yy}=\mu_{yy}=-2$, $\mu_{zz}=\varepsilon_{zz}=-2.5$, and $d=\frac{3}{4}\lambda$ and for another one with parameters given by (b) $\mu_{xx}=\varepsilon_{xx}=-0.5$, $\varepsilon_{yy}=\mu_{yy}=-2$, $\mu_{zz}=\varepsilon_{zz}=-2.5$, and $d=\frac{7}{4}\lambda$. (c) Tr(T) as a function of K_x within the GSW region for the system studied in Fig. 1(a). (d) Tr(T) as a function of K_x within the GSW region for the system studied in Fig. 1(b).

in Fig. 1(a). Obviously, the above set of parameters makes $\mathrm{Tr}(T_{TE})<-2$ and, in turn, $\mathrm{Tr}(T_{TM})<-2$, for all K_x values.

The above analysis also helps us to understand why the $m=1$ Bragg gap is the *only* possibility. For the $m\neq 1$ case, similar analysis indicates that $k_{2z}d_2$ must develop from an angle within $[m\pi,(m+1)\pi]$ to 0 inside the whole GSW region. Therefore, the function $\sin k_{2z}d_2$ must change its sign *more than one time*, so that it is *impossible* to completely destroy the oscillation of Tr(T) inside the GSW region, as we did in the $m=1$ case.

Numerical calculations were performed to verify the above analysis. We have realized an $m=3$ Bragg gap by adopting the set of parameters $\mu_{xx}=\varepsilon_{xx}=-0.5$, $\varepsilon_{yy}=\mu_{yy}=-2$, $\mu_{zz}=\varepsilon_{zz}=-2.5$, $d_1=\frac{1}{4}\lambda$, and $d_2=\frac{7}{4}\lambda$ and have depicted $|\mathrm{Tr}(T)|$ in Fig. 1(b). While we do get $|\mathrm{Tr}(T)|>2$ within both the PW and SPP regions, we find Tr(T) to oscillate from a negative value to a positive one in the GSW region, indicating that guided modes must appear [as $|\mathrm{Tr}(T)|\leq 2$].

Our analysis is also intimately related to the phase argument given by Shadrivov *et al.* In Ref. [11], the authors argued that the condition for the existence of a waveguide mode in a single air/metamaterial/air system is that the total phase accumulation ϕ_{total}, which is twice the sum of the propagating phase ϕ_P and the reflecting phase ϕ_R, should be a multiple of 2π. In Figs. 2(a) and 2(b), we plot $\phi_P[=-k_{2z}d_2]$, ϕ_R, and $\phi_{total}[=2(\phi_P+\phi_R)]$ as functions of K_x in the GSW regions for the two model systems that we studied. Indeed, we find that ϕ_R is always inside $(0,-\pi)$ as pointed out by Shadrivov *et al.* [11]. On the other hand, while the $m=1$ mode can help restrict ϕ_{total} inside a region $(-2\pi,-4\pi)$ so that no guided mode exists, the $m=3$ mode *cannot*. The reason is simply that, for the latter case, ϕ_P starts from an angle located inside $(-3\pi,-4\pi)$, as we have analyzed, and develops towards 0 as K_x increases. As a result, ϕ_{total} inevitably passes -4π and -6π at two K_x values [see Fig. 2(b)], generating guided modes. As a comparison, we present in Figs. 2(c) and 2(d) expanded views of the calculated Tr(T) in the GSW regions for the two model systems. Indeed, while we find that the condition $\mathrm{Tr}(T)<-2$ is satisfied within the whole GSW region for the $m=1$ case, Tr(T) goes into $[-2,2]$ at two K_x intervals for the $m=3$ case, manifesting the existences of two passbands. It is worthy noting that the centers of the two pass bands predicted by our analysis coincide well with the points where $\phi_{total}=-4\pi$, -6π.

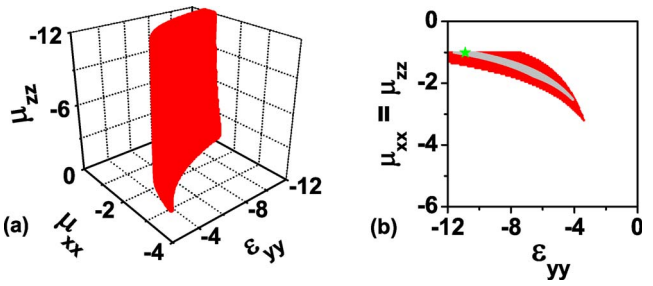

FIG. 3. (Color online) (a) Phase diagram of μ_{xx}, ε_{yy}, and μ_{zz} supporting a 2D complete PBG by analyzing Eq. (2). (b) Phase diagrams of $\mu_{xx}(=\mu_{zz})$ and ε_{yy} supporting a 2D complete PBG obtained by different methods. The dark region (red color online) is obtained by numerically analyzing Eq. (2), the solid star is obtained by solving the analytical criteria (5), (8), (11), and (14), and the light gray region is obtained by solving the relaxed analytical criteria (5), (8), (11′), and (14′) with $\delta_1=0.14$ and $\delta_2=0.27$. Here, we set $d_1=1.5\lambda/2\pi$ and $d_2=1.4\lambda/2\pi$.

C. Situation of $\vec{\varepsilon}$, $\vec{\mu}>0$

Similar arguments show that a complete PBG *cannot* exist in 1D periodic structures containing only *ordinary* materials (i.e., all elements of $\vec{\varepsilon}$ and $\vec{\mu}$ are positive). First, we find that Tr(T) tends to $+\infty$ as $K_x\rightarrow+\infty$, indicating that *we need to ensure* $\mathrm{Tr}(T)>2$ *for all* K_x *to realize a complete PBG*. The criterion in the PW region is still Eq. (11). In the GSW region, we have

$$\mathrm{Tr}(T)=(e^{-\alpha d_1}+e^{\alpha d_1})\cos k_{2z}d_2+\frac{1}{2}\left(\frac{k_{2z}}{\mu_{xx}\alpha}-\frac{\mu_{xx}\alpha}{k_{2z}}\right)\times\sin k_{2z}d_2(e^{-\alpha d_1}-e^{\alpha d_1}), \quad (16)$$

with $k_{1z}=i\alpha$. Similar to the arguments in the last subsection, we know that $k_{2z}d_2$ decreases from an angle located inside $(\pi,2\pi)$ to zero as K_x increases. Therefore, there must be a particular K_x value where $k_{2z}d_2$ is equal to π. However, this K_x value unfortunately leads to $\mathrm{Tr}(T)=-2(e^{-\alpha d_1}+e^{\alpha d_1})<-2$, violating our requirement of $\mathrm{Tr}(T)>2$. As a result, Tr(T) must oscillate from $+\infty$ to a negative value, leading to passbands.

III. PHASE DIAGRAMS AND PHOTONIC BAND STRUCTURES

Now we compare our results with the isotropic case studied by Shadrivov *et al.* [11]. To avoid using two many vari-

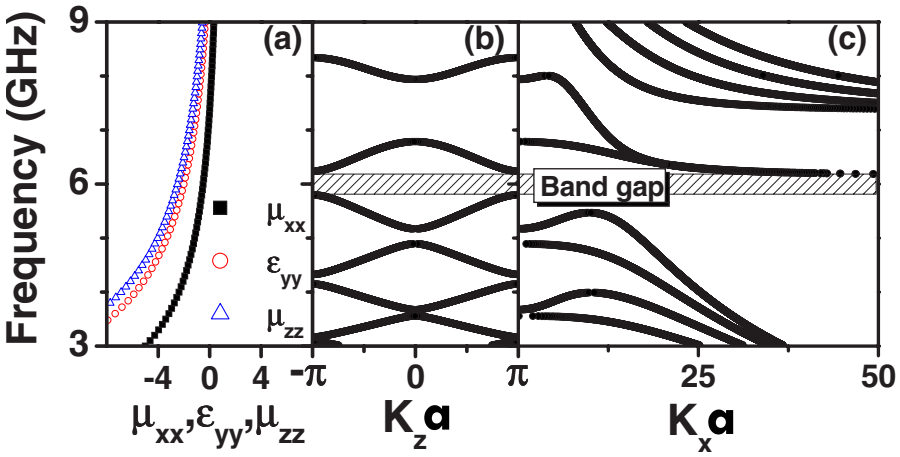

FIG. 4. (Color online) (a) μ_{xx}, ε_{yy}, and μ_{zz} of the anisotropic metamaterial as functions of frequency. Calculated photonic band structures for waves traveling along (b) the periodic direction and (c) the lateral direction, for the 1D periodic system with material parameters shown in (a).

ables, we set $d_1=1.5\lambda/2\pi$ and $d_2=1.4\lambda/2\pi$, just as Ref. [11]. We have numerically analyzed Eq. (2) and present a phase diagram in Fig. 3(a) to depict the permitted values of μ_{xx}, ε_{yy}, and μ_{zz} that guarantee $|\mathrm{Tr}[T_{TE}(\omega,K_x)]|>2$ for all K_x. If we pick up those points satisfying $\mu_{zz}=\mu_{xx}$ from Fig. 3(a) and project them onto a 2D diagram of μ_{xx} $(=\mu_{zz})$ versus ε_{yy} in Fig. 3(b), we find that the obtained phase diagram *exactly* recovers that of the isotropic case shown in Fig. 3 of Ref. [11], as expected. Obviously, the anisotropy here provides with us a wider parameter region than the isotropic LHM layer case adopted by Shadrivov *et al.* [11], if one only wants to realize a 2D complete PBG [22].

To demonstrate the validity of our analytical criteria, we have compared the parameter region obtained by solving our analytical criteria with that by numerically analyzing Eq. (2). For simplicity we only consider the isotropic case. Solving the criteria (5), (8), (10), and (14) with $\mu_{xx}=\mu_{zz}$, we found a solution $\mu_{xx}=\mu_{zz}=-1.0097\varepsilon_{yy}=-10.886$ and plot it as a solid star in Fig. 3(b). This solution is located well inside the "exact" parameter region obtained numerically. As we have pointed out, the analytical criteria that we obtained are sufficient conditions to realize a 2D complete PBG, but not necessary ones. In particular, the conditions (11) and (14) are overly strict. If we relax those two conditions as

$$\left|\frac{\omega}{c}d_1-\sqrt{\varepsilon_{yy}\mu_{xx}}\frac{\omega}{c}d_2+\pi\right|<\delta_1, \tag{11'}$$

$$\left|\sqrt{\frac{\mu_{xx}^2(\mu_{zz}\varepsilon_{yy}-1)}{1+\mu_{zz}\mu_{xx}}}\frac{2d_2}{\lambda}-1\right|<\delta_2, \tag{14'}$$

where δ_1 and δ_2 are two small positive numbers, we can then find an expanded parameter region. For example, we have solved the relaxed analytical criteria (5), (8), (11′), and (14′) with $\delta_1=0.14, \delta_2=0.27$. The obtained parameter region is shown in Fig. 3(b) as a gray area, which is still inside the "exact" parameter region obtained numerically. However, one should be careful not to choose too large values for δ_1 and δ_2, since the relaxed conditions (11′) and (14′) are not rigorous anyway.

Since all LHM samples are highly dispersive [23,24], we now consider a system consisting of a dispersive anisotropic LHM layer with $\overleftrightarrow{\varepsilon}$ and $\overleftrightarrow{\mu}$ given by

$$\mu_{xx}=\varepsilon_{xx}=1-\frac{54}{f^2},\quad \varepsilon_{yy}=\mu_{yy}=1-\frac{108}{f^2},$$

$$\mu_{zz}=\varepsilon_{zz}=1-\frac{126}{f^2}, \tag{17}$$

where f denotes the frequency measured in GHz. The frequency dependences of these parameters are shown in Fig. 4(a). At $f=6$ GHz, we find that $\mu_{xx}=\varepsilon_{xx}\approx-0.5$, $\varepsilon_{yy}=\mu_{yy}\approx-2$, $\mu_{zz}=\varepsilon_{zz}\approx-2.5$, and $\lambda_0=50$ mm. If we further set $d_1=\frac{1}{4}\lambda_0$ and $d_2=\frac{3}{4}\lambda_0$, we find that this set of parameters is just what we have used in Fig. 1(a) [Eq. (15)]. We then employ these parameters to calculate the photonic band structures of our system for two particular directions—along the periodic direction (i.e., set $K_x=0$) and along the lateral direction (i.e., set $K_z=0$)—and show the results in Figs. 4(b) and 4(c), respectively. As expected, photonic band gaps appear simultaneously around 6 GHz in both spectra. We can easily identify that the PBG along the periodic direction [Fig. 4(b)] is induced by Bragg scattering. In addition, we note that $|K_z a|=\pi$ inside the gap, consistent with Eqs. (7) and (8) dictating that the Bragg gap must be a mode with $m=1$.

On the other hand, the photonic band structure for light traveling along the lateral direction is quite complicated, which obscures our understanding of the gap opening mechanism. To gain a clearer understanding, we replot the band structure in Fig. 5, with a light line $(K_x=\omega/c)$ added. In addition, we adopt dark (bright) regions in Fig. 5 to represent the situations where the EM waves are evanescent (propagating) inside the anisotropic metamaterial. With the help of these auxiliary tools, we can easily identify the three regions (i.e., the PW, GSW, and SPP regions), which we defined in Sec. II B. We find that the spectra in different regions can be traced back to different origins. For example, the band structures within the GSW and SPP regions coincide excellently with the dispersion relations of the guided surface waves and surface plasmon polaritons calculated for a *single* anisotropic LHM slab (denoted by open triangles and open stars, respectively). This is understandable since evanescent waves in air decay so rapidly that coupling between different slabs can be neglected as K_x is large enough.

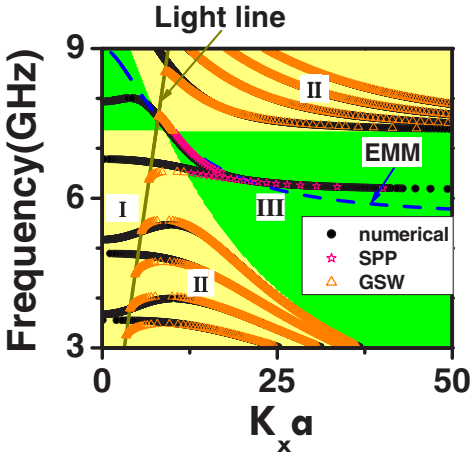

FIG. 5. (Color online) Photonic band structure (solid circles) of the 1D periodic system for waves traveling along the lateral direction, compared with the dispersion relations of the guided surface waves (open triangles, orange color online) and the surface plasmon polaritons (open stars, pink color online) for a single anisotropic LHM slab. Electromagnetic waves inside the anisotropic metamaterial are evanescent in the dark (green color online) region and are propagating inside the bright (yellow color online) region. The dashed line (blue color online) represents the dispersion relation given by the effective media model.

However, deviations exist when approaching the light line of air, where evanescent waves decay slowly in air so that the coupling between slabs becomes important. For such a situation, we find that the effective medium model (EMM) works well. For light traveling along the lateral direction and with a TE polarization, in the long-wavelength limit ($k_{1z}d_1 \ll 1, k_{2z}d_2 \ll 1$), we find that the system can be viewed as an effective medium with $\varepsilon_{eff}=(d_1+\varepsilon_{yy}d_2)/(d_1+d_2)$ and $\mu_{eff}=(d_1+d_2)/(d_1+\mu_{xx}^{-1}d_2)$, which shows that ε_{eff} is a volume average of individual dielectric constants and the inverse of μ_{eff} corresponds to a volume average of the inverse of permeability. The dashed line in Fig. 5 represents the dispersion of the EMM,

$$k_x = \sqrt{\varepsilon_{eff}(\omega)\mu_{eff}(\omega)}\frac{\omega}{c}, \tag{18}$$

which coincides perfectly with the realistic band structure in the region where the long-wavelength limit is reached.

Now that we know the origins of all those photonic modes in different regions, we then gain a deeper understanding of the mechanism to build a complete PBG. To do so, we need to suppress simultaneously the effective medium mode, the GSW modes, and the SPP modes and to create an $m=1$ Bragg gap along the periodic direction within a given frequency band. In fact, our condition (5) is nothing but to suppress the SPP modes; our condition (14) is sufficient to destroy the GSW modes; the condition (8) helps us to create an $m=1$ Bragg gap; and the condition (11) ensures that the Bragg gap is not closed within the whole PW region.

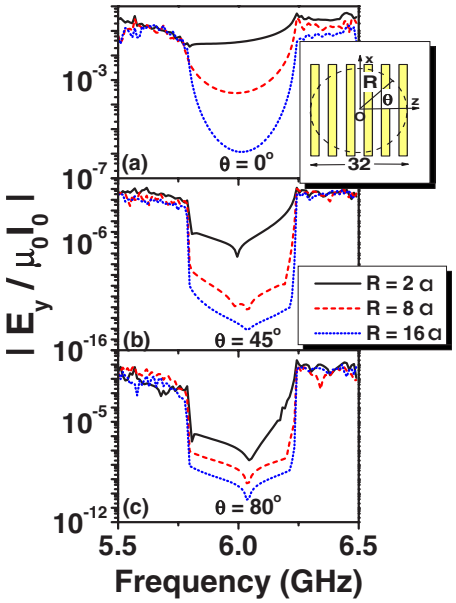

FIG. 6. (Color online) $|E_y/\mu_0 I_0|$ as functions of the frequency, measured at positions given by $\vec{r}=R(\cos\theta\hat{z}+\sin\theta\hat{x})$ [see the inset to (a)], where θ is fixed as (a) 0°, (b) 45°, and (c) 80° and R is fixed as $2a$ (solid lines), $8a$ (dashed lines), and $16a$ (dotted lines).

IV. ILLUSTRATIONS OF THE COMPLETE PBG EFFECT

We present some numerical results to illustrate the complete PBG effects. We consider a layered system with 32 double-layer unit cells, with structural parameters $d_1=\frac{1}{4}\lambda_0$ and $d_2=\frac{3}{4}\lambda_0$ ($\lambda_0=50$ mm) and material parameters given by Eq. (17). An infinitely long line current source, with current distribution given by $\vec{j}(r,t)=\mu_0 I_0\delta(x)\delta(z)e^{-i\omega t}\hat{y}$, is placed at the center of the system. Extending the Green-function method developed previously for a single-slab case [25] to the present multilayer case, we are able to calculate the electric field at an arbitrary point within the structure. For three typical directions $\theta=0°$, 45°, 80° [26], with θ being the azimuthal angle, we have calculated the electric field E_y as functions of frequency $f(=\omega/2\pi)$, at positions determined by $\vec{r}=R(\cos\theta\hat{z}+\sin\theta\hat{x})$ [see the inset to Fig. 6(a)]. The ampli-

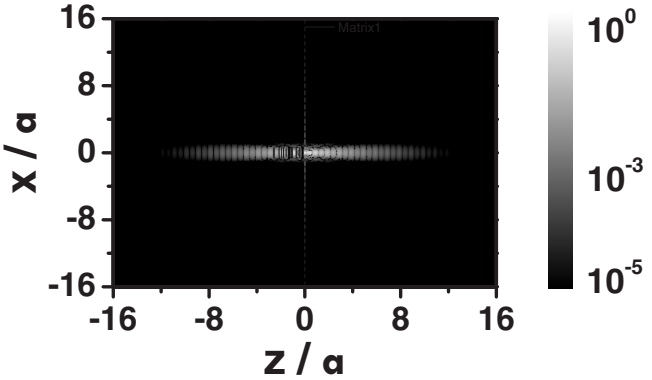

FIG. 7. Electric field $|E_y/\mu_0 I_0|$ distribution inside the 32-unit-cell sample with an infinitely long line current source placed at the origin working at $f=6$ GHz.

tudes of the normalized electric fields $|E_y/\mu_0 I_0|$, which are proportional to the transmission rates, are depicted versus frequency f in Figs. 6(a)–6(c), for the three angles correspondingly. For all three directions considered, the diminished transmissions within a common frequency regime (5.8–6.17 GHz) have unambiguously demonstrated that a 2D complete PBG does open there. In particular, when the observation point moves far away (i.e., R increases), the transmission rate decreases drastically while the gap edge is sharpened. These are typical characteristics of a PBG.

At the central gap frequency $f=6$ GHz, we employed the Green-function method to calculate the electric field distribution inside the same system. From the field distribution recorded in Fig. 7 [26], we see clearly that waves radiated from the line source *cannot* propagate along *any* direction inside the structure, demonstrating that we have realized a 2D complete PBG in such a structure. Considering the duality between $\overleftrightarrow{\varepsilon}$ and $\overleftrightarrow{\mu}$ of the present system, it is natural to conclude that the gap is a 2D polarization-independent complete one.

V. CONCLUSIONS

To summarize, we have demonstrated the possibilities of realizing a 2D polarization-independent complete PBG in a 1D periodic structure with a double-layer unit cell consisting of an air layer and an anisotropic (transparent) LHM layer. Through analyzing the trace of the transfer matrix function, we have derived a set of criteria imposed on the materials and structures, in order to realize a 2D complete PBG. Compared with the 1D isotropic periodic left-handed structures studied previously, we find that the present system offers a wider permitted parameter region to realize a 2D complete PBG. We have discussed the underlying physics of the mechanism and employed several examples to illustrate the complete PBG effects.

ACKNOWLEDGMENTS

We thank Professor C.T. Chan for many stimulating discussions. This work was supported by the National Basic Research Program of China (Grant No. 2004CB719800), the NSFC (Grant No. 10504003), Shanghai Science and Technology Committee (Grants Nos. 05PJ14021 and 5JC14061), Fok Ying Tung Education Foundation, and PCSIRT.

[1] E. Yablonovitch, Phys. Rev. Lett. **58**, 2059 (1987).
[2] S. John, Phys. Rev. Lett. **58**, 2486 (1987).
[3] J. D. Joannopoulos, P. R. Villeneuve, and S. Fan, Nature (London) **386**, 143 (1997).
[4] K. M. Ho, C. T. Chan, and C. M. Soukoulis, Phys. Rev. Lett. **65**, 3152 (1990).
[5] E. Yablonovitch, T. J. Gmitter, and K. M. Leung, Phys. Rev. Lett. **67**, 2295 (1991).
[6] J. N. Winn, Y. Fink, S. Fan, and J. D. Joannopoulos, Opt. Lett. **23**, 1573 (1998).
[7] Y. Fink, J. N. Winn, S. Fan, C. Chen, J. Michel, J. D. Joannopoulos, and E. L. Thomas, Science **282**, 1679 (1998).
[8] V. C. Veselago, Sov. Phys. Usp. **10**, 509 (1968).
[9] D. R. Smith, W. J. Padilla, D. C. Vier, S. C. Nemat-Nasser, and S. Schultz, Phys. Rev. Lett. **84**, 4184 (2000).
[10] J. Li, L. Zhou, C. T. Chan, and P. Sheng, Phys. Rev. Lett. **90**, 083901 (2003).
[11] I. V. Shadrivov, A. A. Sukhorukov, and Y. S. Kivshar, Phys. Rev. Lett. **95**, 193903 (2005); Proc. SPIE **6038**, 60380Z (2005).
[12] I. V. Shadrivov, A. A. Sukhorukov, and Y. S. Kivshar, Phys. Rev. E **67**, 057602 (2003).
[13] L. Zhou, C. T. Chan, and P. Sheng, Phys. Rev. B **68**, 115424 (2003).
[14] L. B. Hu and S. T. Chui, Phys. Rev. B **66**, 085108 (2002).
[15] D. R. Smith and D. Schurig, Phys. Rev. Lett. **90**, 077405 (2003).
[16] Y. J. Feng, X. H. Teng, Y. Chen, and T. Jiang, Phys. Rev. B **72**, 245107 (2005).
[17] S. Wang and L. Gao, Eur. Phys. J. B **48**, 29 (2005).
[18] Here we adopt a convention to take the positive root of the square-root function and note that the final results do not change if one chooses a different convention [see, e.g., J. B. Pendry, Phys. Rev. Lett. **85**, 3966 (2000)].
[19] This inequality is violated if we have $\Delta=-1$ at some particular K_x value. However, the criteria that we obtained have explicitly excluded this possibility which is unfavorable to create a complete PBG. In the SPP region, we find that $\Delta \in (0, -1/\sqrt{\mu_{xx}\mu_{zz}})$ and thus Eq. (5) ensures that $\Delta \neq -1$ within this region; in the GSW region, Δ is a purely imaginary number; in the PW region, we find that $\Delta \in (-\infty, -\sqrt{\varepsilon_{yy}/\mu_{xx}})$ and thus Eq. (10) ensures that $\Delta \neq -1$ within this region.
[20] H. T. Jiang, H. Chen, H. Q. Li, Y. W. Zhang, and S. Y. Zhu, Appl. Phys. Lett. **83**, 5386 (2003).
[21] For the $\bar{n}=0$ gap, we have $\mathrm{Tr}(T)>+2$ for $K_x=0$ (see Ref. [10]). On the other hand, we have $\mathrm{Tr}(T)\to-\infty$ as $K_x\to\infty$ [see the discussions after Eq. (4)]. Therefore, passbands [i.e., $|\mathrm{Tr}(T)|\leq 2$] must appear as K_x changes from 0 to ∞.
[22] If one is interested in a 3D complete band gap, the isotropic system seems superior than the present anisotropic one, since the 2D complete gap in the former case automatically becomes a 3D one due to the symmetry between x and y directions.
[23] R. A. Shelby, D. R. Smith, S. C. Nemat-Nasser, and S. Schultz, Appl. Phys. Lett. **78**, 489 (2001).
[24] R. A. Shelby, D. R. Smith, and S. Schultz, Science **292**, 77 (2001).
[25] L. Zhou and C. T. Chan, Appl. Phys. Lett. **86**, 101104 (2005).
[26] There are some intrinsic numerical convergence problems for calculating the case with $\theta=90°$, so that we adopt an angle slightly different from 90°. We also skipped calculating those points with $\theta=90°$ in Fig. 7 due to the same reason.